

APPENDIX NUCLEAR STRUCTURE

1. Spherical Shell Model

The stability of certain combinations of neutrons and protons was pointed out by Elsasser¹ in 1934. Stability for light nuclei with N or Z values of 2 (⁴He), 8 (¹⁶O), and 20 (⁴⁰Ca) became well known, and in 1948 Mayer² observed strong evidence for additional "magic numbers" at 50 and 82 for protons, and 50, 82, and 126 for neutrons. Mayer and Jensen³ explained this in terms of a "shell model", where nucleons moved in a spherically symmetric potential well. This potential is most commonly taken as a harmonic oscillator of the form

$$V(r) = -V_0 \left[1 - (r/R)^2 \right], \quad (1)$$

where $V(r)$ is the potential at a distance r from the center of the nucleus and R is the nuclear radius. The resulting quantum states can be characterized by n , the principal quantum number related to the number of radial nodes in the wave function, and by l , the orbital angular momentum of the particle. By analogy to atomic spectroscopy, states with $l = 0, 1, 2, 3, 4, 5, 6, \dots$ are designated as $s, p, d, f, g, h, i, \dots$, respectively. The states are identified by as $1s, 2f, 3p$, etc, where, unlike in atomic spectroscopy, n is defined so that each state has $n-1$ radial nodes.

The solution of the Schrödinger equation for the isotropic harmonic oscillator gives the level energies

$$E = \hbar \omega_0 [2(n-1) + l] + E_0, \quad (2)$$

where

$$\omega_0 = \left(\frac{2V_0}{MR^2} \right)^{1/2}, \quad (3)$$

M is the nucleon mass, and $E_0 = 3/2 \hbar \omega_0$. Here states with the same value of $N = 2(n-1) + l$ are degenerate, and states of a given energy must all have either even or odd values of l . Thus, degenerate states must have the same parity.

Mayer⁴ and Haxel *et al*⁵ showed that the interaction between the intrinsic angular momentum (spin) of the particles and their total angular momentum would split the orbitals into two substates with $l \pm 1/2$ (e.g. $1p_{1/2}$ and $1p_{3/2}$). These states are no longer degenerate, and it was shown that if the "spin-orbit" interaction is of the same order as the spacing between oscillator shells, and states with $j = l + 1/2$ are more stable than states with $j = l - 1/2$, then the magic numbers can be reproduced. The evolution of shell model states from the harmonic oscillator model is depicted in Figure 1.

2. Collective Model

The shell model succeeds in describing nuclei near the magic numbers, but it fails to adequately describe nuclei outside the closed shells. This may be attributed to a breakdown in the assumption of spherical symmetry. Rainwater⁶ proposed that, in odd-A nuclei, the motion of the odd nucleon could polarize the even-even core allowing all nucleons to move collectively, thus increasing the static electric quadrupole moments and enhancing quadrupole transition ($E2$) rates. The implications of spheroidal rather than spherical shape were studied by Bohr and Mottelson⁷ who developed a collective model for nuclei.

For a spheroidal nucleus, the orbital angular momentum of the odd nucleon is no longer conserved. Since total angular momentum for the nuclear system must be conserved, the core must have angular momentum coupled to that of the odd nucleon. Addition of more nucleons outside the closed shells can

¹ W. Elsasser, *J.Phys. Rad.* **5**, 625 (1934).

² M.G. Mayer, *Phys. Rev.* **74**, 235 (1948).

³ M.G. Mayer and J.H.D. Jensen, *Elementary Theory of Nuclear Shell Structure*, John Wiley & Sons, Inc., New York (1955).

⁴ M.G. Mayer, *Phys. Rev.* **78**, 16 (1950).

⁵ O. Haxel, J.H.D. Jensen, and H.E. Suess, *Z. Physik* **128**, 295 (1950).

⁶ L.J. Rainwater, *Phys. Rev.* **79**, 432 (1950).

⁷ A. Bohr and B.R. Mottelson, *Dan. Mat.-Fys. Medd.* **27**, No. 16 (1953); and "Collective Nuclear Motion and the Unified Model", *Beta and Gamma Ray Spectroscopy*, K. Siegbahn, editor, North Holland, Amsterdam (1955).

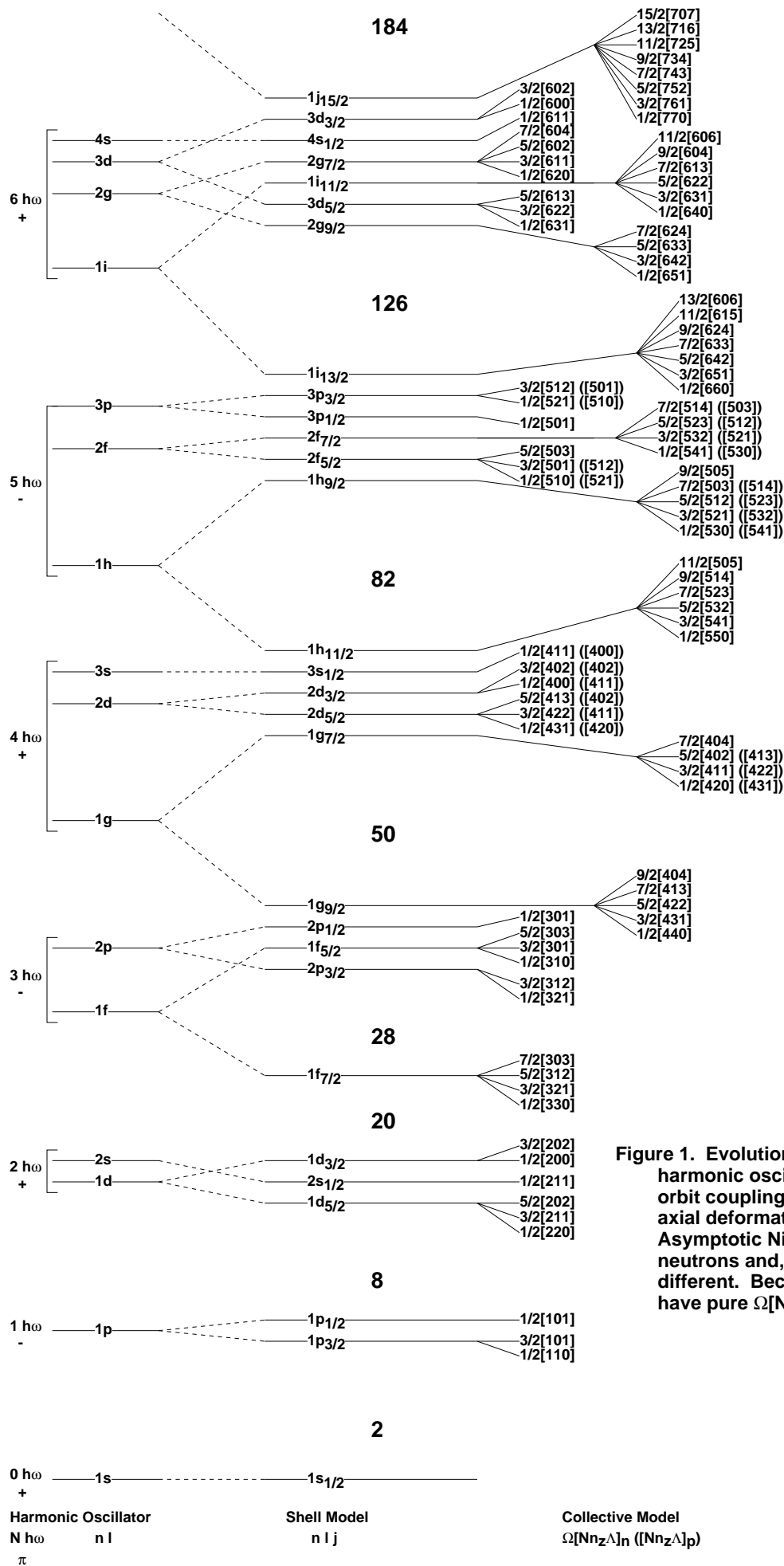


Figure 1. Evolution of nuclear models from the harmonic oscillator model, adding strong spin-orbit coupling to obtain the shell model, and axial deformation to give the collective model. Asymptotic Nilsson configurations are given for neutrons and, in parentheses, for protons when different. Because of mixing, very few states have pure $\Omega[Nnz\Lambda]$ configurations.

form spheroidal nuclei whose angular momentum states reflect the coherent motion of all nucleons rather than just a few nucleons moving in single-particle shell model orbitals. The quantization of this coherent motion forms the basis of the collective model.

This collective motion can be quantized by assuming that the even-even core is an incompressible liquid and quantizing the classical hydrodynamical equations that describe its oscillations. Borrowing from the well-known analysis of rotational states in symmetric-top molecules, we expect the level energy relation

$$E = \hbar^2 \frac{[J(J+1) - K^2]}{2\mathcal{I}_1} + \frac{\hbar^2 K^2}{2\mathcal{I}_3} \quad (4)$$

where $[J(J+1)]^{1/2}\hbar$ is the total angular momentum of the nucleus, and $K\hbar$ is the component of angular momentum along the symmetry axis of the nucleus, as shown in Figure 2. \mathcal{I}_1 and \mathcal{I}_3 are the moments of inertia perpendicular and parallel to the symmetry axis, respectively. For low-lying rotational bands in even-even nuclei, $K=0$ and Eq. (4) reduces to

$$E = \hbar^2 \frac{[J(J+1)]}{2\mathcal{I}_1} . \quad (5)$$

States with $K \neq 0$ arise when one or more pairs of nucleons are broken and unpaired nucleons are excited to higher shell-model states. Low-lying rotational levels with $K=0$ are characterized by a sequence of states with $J = 0, 2, 4, 6, 8, \dots$ and positive parity, often referred to as the ground-state (GS) band. An example of the GS band for ^{152}Sm is shown in Figure 3. Excited vibrational states of three kinds are also shown for ^{152}Sm in Figure 3. The β -vibration preserves spheroidal symmetry, and the γ -vibration goes through an ellipsoidal symmetry. The octupole vibration produces a low-lying $J^\pi=3^-$ state in spherical nuclei, but can also couple to core quadrupole excitations in deformed nuclei to give a family of low-lying states with $J^\pi=1^-, 2^-, 3^-, 4^-,$ and 5^- .

3. Deformed Shell Model

A unified model for the effect of deformation on shell-model states has been developed by Nilsson¹ and by Mottelson and Nilsson². The deformation breaks the $2j + 1$ degeneracy of the spherical shell-model states. Asymptotic quantum numbers needed to describe these states are shown in Figure 2. In addition to K , they include N , the total oscillator shell quantum number; n_z , the number of oscillator quanta in the z direction; M , the projection of total angular momentum J on the laboratory axis; R , the angular momentum from the collective motion of the nucleus; Ω , the projection of total angular momentum j (orbital l plus spin s) of the odd nucleon on the symmetry axis; and Λ , the projection of angular momentum along the symmetry axis where $\Omega = \Lambda + \Sigma$ and Σ is the projection of intrinsic spin along the symmetry axis. Levels are labeled by the asymptotic quantum numbers $\Omega^\pi[Nn_z\Lambda]$. The Nilsson orbitals which derive from the axially deformed harmonic oscillator potential, labeled as described by Davidson³, are shown in Figure 1. A more realistic calculation can be performed using a Woods-Saxon potential

$$V(r) = \frac{V_0}{1 + \exp\left(\frac{r-R}{a}\right)} , \quad (6)$$

where $a \approx 0.67$ fm. Considerable mixing of Nilsson configurations with $\Delta\Omega=0$, $\Delta N=2$, and similar excitation energies may occur leaving only Ω as a good quantum number. Representative Nilsson level diagrams, for various mass regions and deformations, calculated as described by Bengtsson and Ragnarsson⁴, are shown in Figures 4-14. In these figures, single-particle energies are plotted in units of the oscillator frequency

$$\hbar\omega_0 = 41A^{-1/3} \text{ MeV} \quad (7)$$

as a function of deformation ε_2 , with ε_4 chosen as described in the figure captions. The Nilsson quadrupole deformation parameter ε_2 can be defined in terms of $\delta = \frac{\Delta R}{R_{r.m.s.}}$ where $R_{r.m.s.}$ is the root mean

¹ S.G. Nilsson, *Dan. Mat.-Fys. Medd.* **29**, No. 16 (1955).

² B.R. Mottelson and S.G. Nilsson, *Phys. Rev.* **99**, 1615 (1955).

³ J.P. Davidson, *Collective Models of the Nucleus*, Academic Press (1968).

⁴ T. Bengtsson and I. Ragnarsson, *Nucl. Phys.* **A436**, 14 (1985).

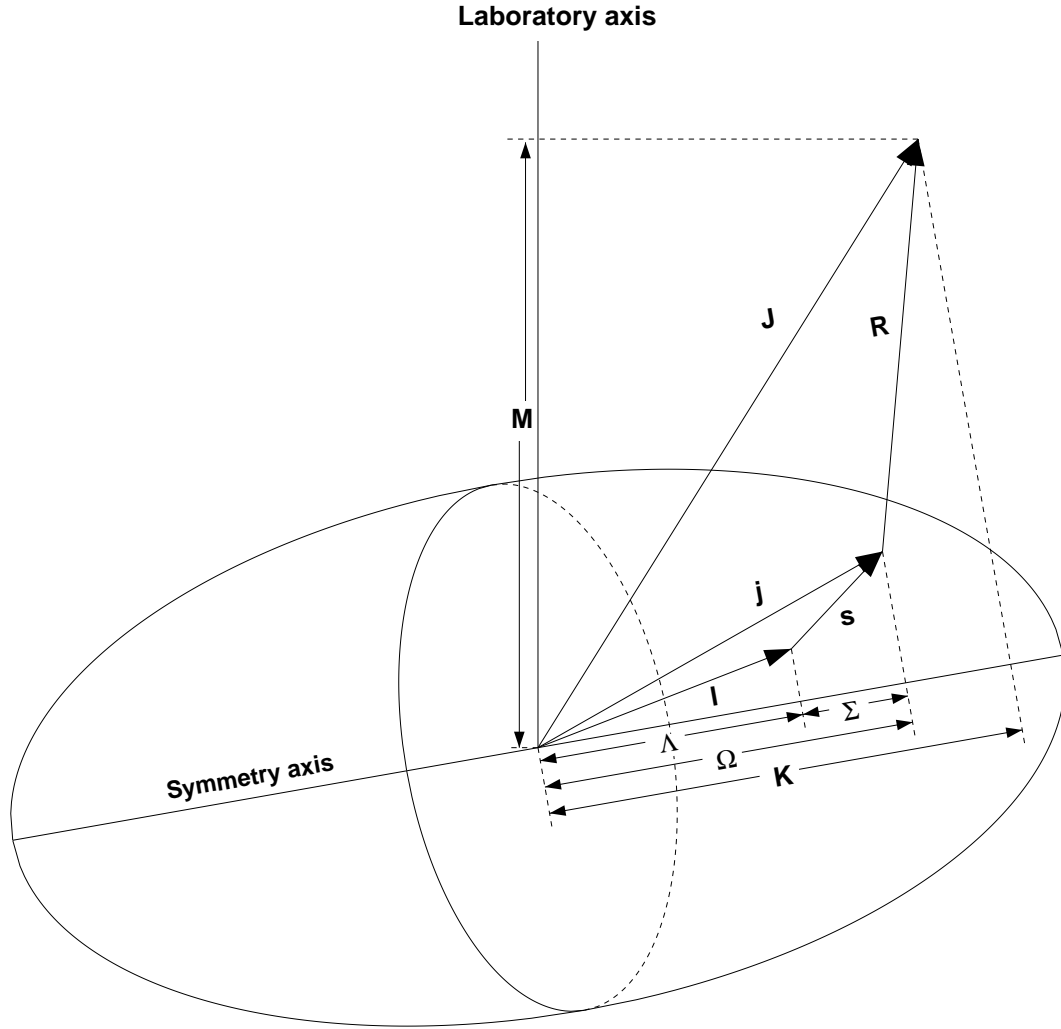


Figure 2. Asymptotic quantum numbers for the deformed shell model

square nuclear radius and ΔR is the difference between the semi-major and semi-minor axes of the nuclear ellipsoid, as¹²

$$\varepsilon_2 = \delta + \frac{1}{6}\delta^2 + \frac{5}{18}\delta^3 + \frac{37}{216}\delta^4 + \dots \quad (8)$$

The deformation parameter β_2 is related to ε_2 by

$$\beta_2 = \sqrt{\pi/5} \left[\frac{4}{3}\varepsilon_2 + \frac{4}{9}\varepsilon_2^2 + \frac{4}{27}\varepsilon_2^3 + \frac{4}{81}\varepsilon_2^4 + \dots \right] \quad (9)$$

The intrinsic quadrupole moment Q_0 (or transition quadrupole moment $Q_T \approx Q_0$) is related to β_2 by

$$Q_0 = \sqrt{16\pi/5} Z e R_0^2 \beta_2. \quad (10)$$

If the partial photon half-life for the E2 transition is known, the experimental transition strength $B(E2)$ is given by

$$B(E2) = \frac{0.05659}{t_{1/2}(E2)(E_\gamma)^5} (eb)^2, \quad (11)$$

¹² K.E.G. Löbner, M. Vetter, and V. Hönl, *Nucl. Data Tables* **A7**, 495 (1970).

where $t_{1/2}(E2)$ is in picoseconds, and E is in MeV. $B(E2)$ is related to Q_0 by

$$B(E2) = B(JK \rightarrow J-2 K) = \frac{5}{16\pi} Q_0^2 \langle JK20 | J-2 K \rangle^2 (eb)^2. \quad (12)$$

Assuming a constant charge distribution in the nucleus, $Q_0=0$ for spherical nuclei, $Q_0>0$ for prolate (football or cigar shaped) nuclei, and $Q_0<0$ for oblate (disk shaped) nuclei. The spectroscopic quadrupole moment Q is related to the intrinsic moment by ¹²

$$Q = Q_0 \frac{3K^2 - J(J+1)}{(J+1)(2J+3)}. \quad (13)$$

For $M1$ transitions, the transition strength $B(M1)$ is given by

$$B(M1) = B(JK \rightarrow J\pm 1 K) = \frac{3}{4\pi} (g_K - g_R)^2 K^2 \langle JK10 | J\pm 1 K \rangle^2 \mu_N^2, \quad (14)$$

where g_K and g_R are nuclear g -factors. The rotational g -factor, g_R , arises from the collective rotation of the core, and is defined as

$$g_R \approx \frac{Z}{A}. \quad (15)$$

The intrinsic g -factor, g_K , arises from the orbital motion of the valence nucleons, and the total magnetic dipole moment is given by

$$\mu = g_R J + (g_K - g_R) \frac{K^2}{J+1} \quad (16)$$

If the partial photon half-life for the $M1$ transition is known, then $B(M1)$ can be calculated from

$$B(M1) = \frac{0.0394}{t_{1/2}(M1) E_\gamma^3} \mu_N^2. \quad (17)$$

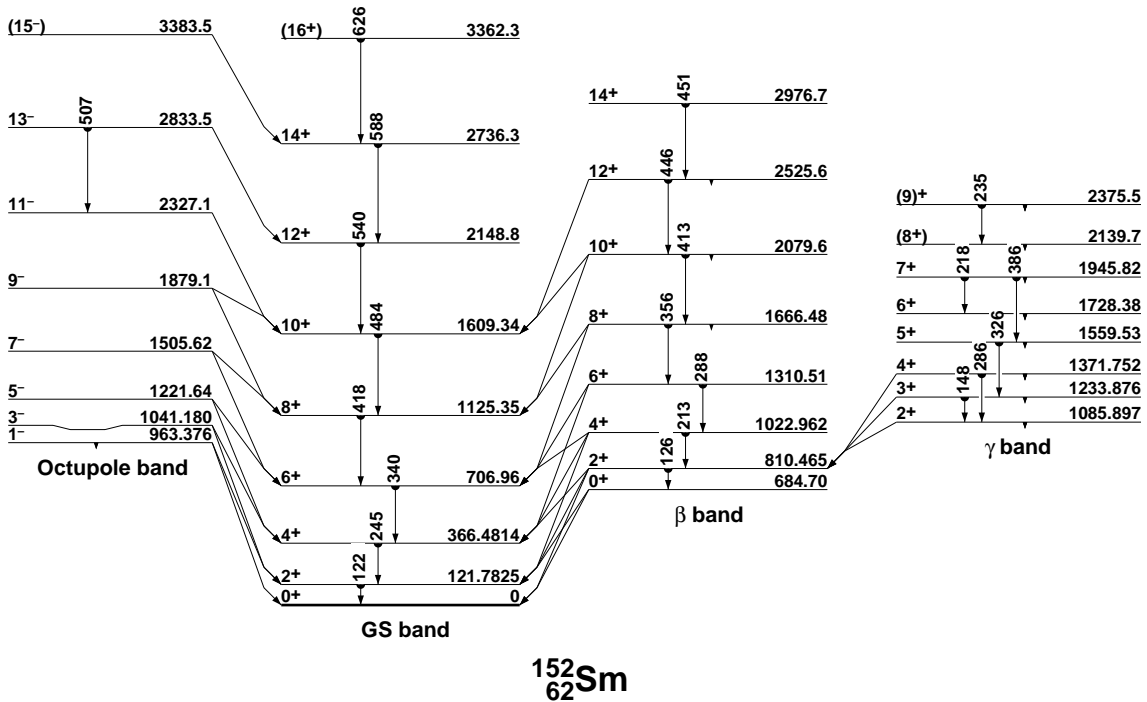


Figure 3. Ground-state, and β -, γ -, and octupole-vibrational bands in ¹⁵²Sm.

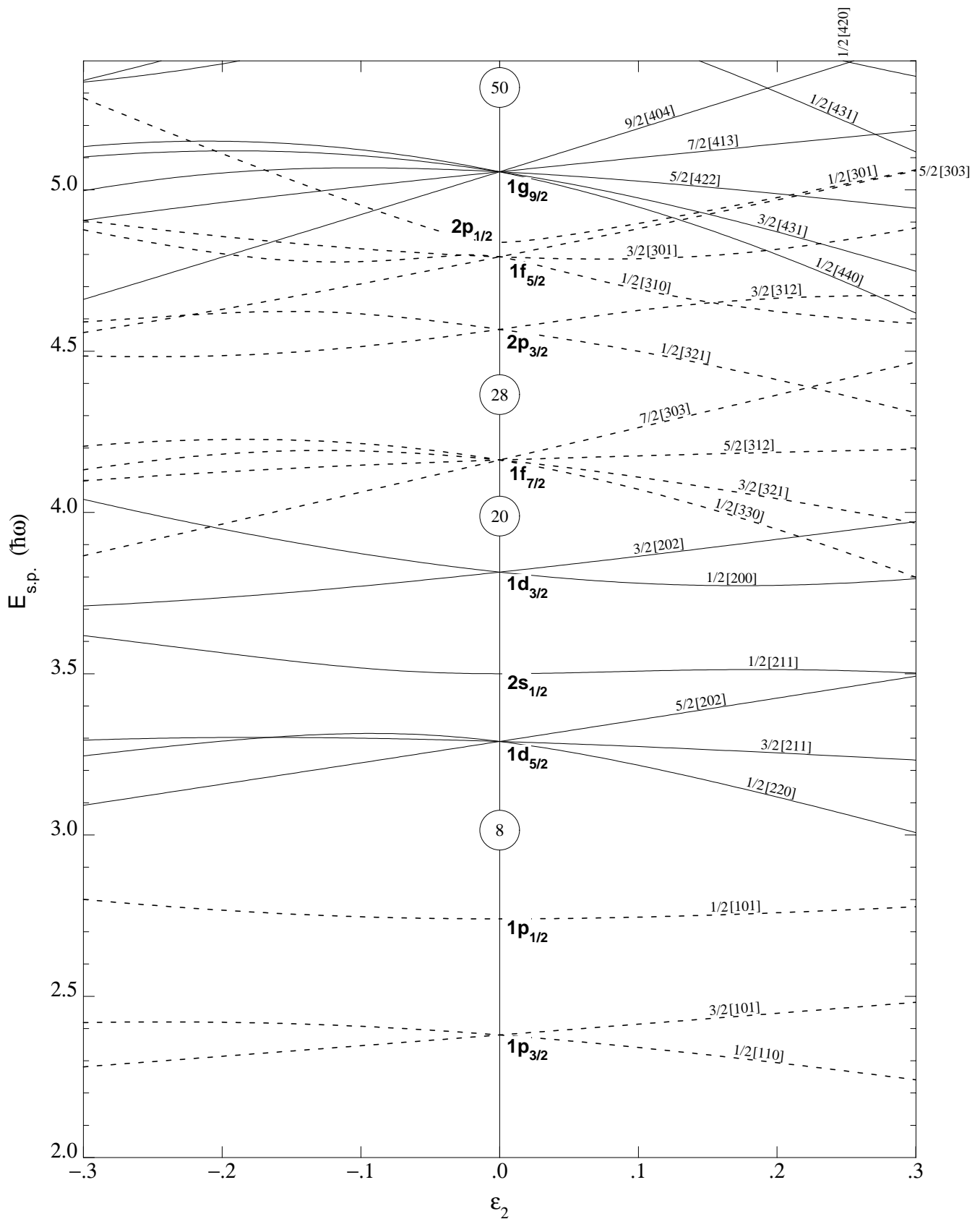


Figure 4. Nilsson diagram for protons or neutrons, $Z, N \leq 50$ ($\epsilon_4 = 0$).

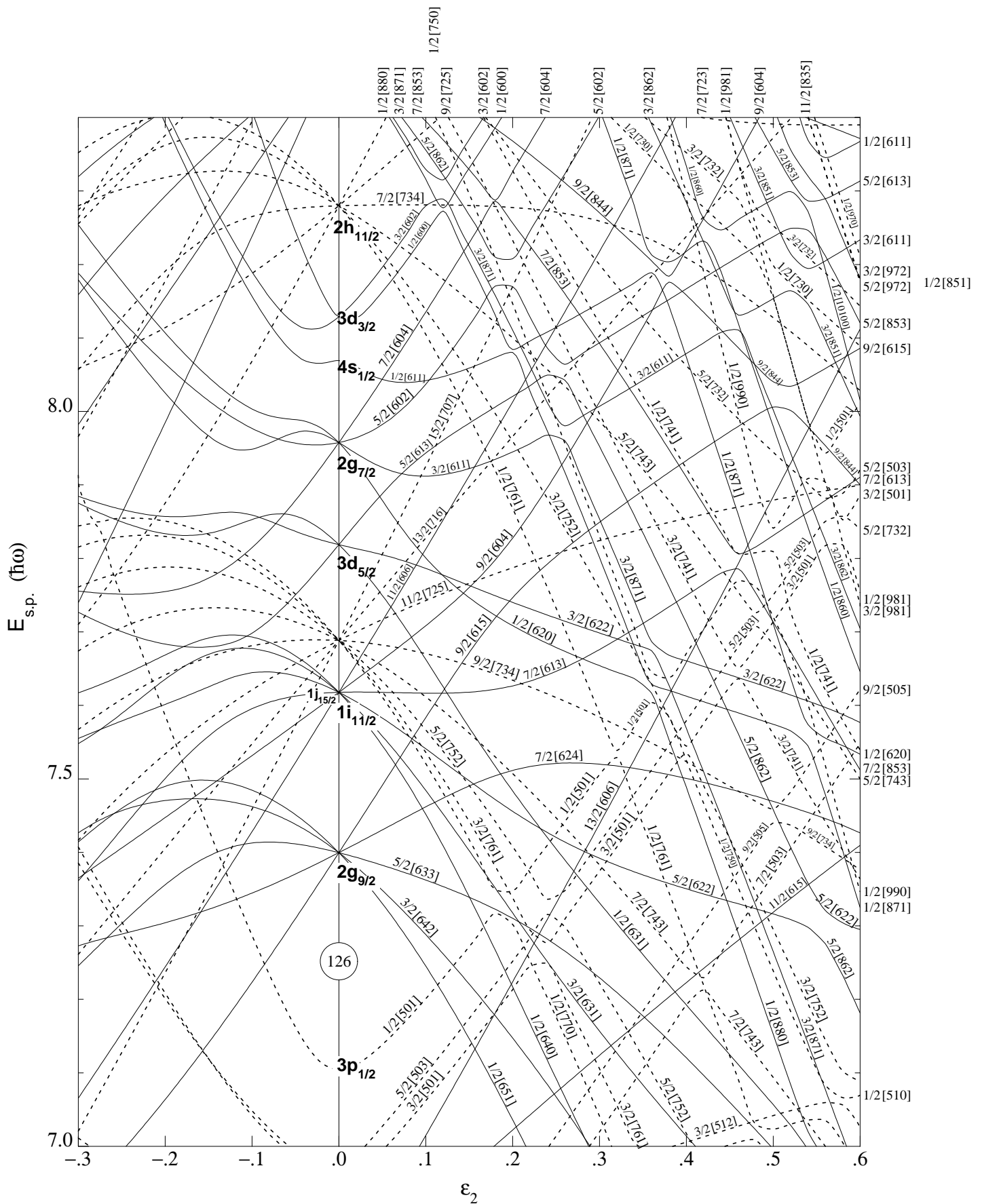


Figure 9. Nilsson diagram for neutrons, $N \geq 126$ ($\epsilon_4 = \epsilon_2^2/6$).

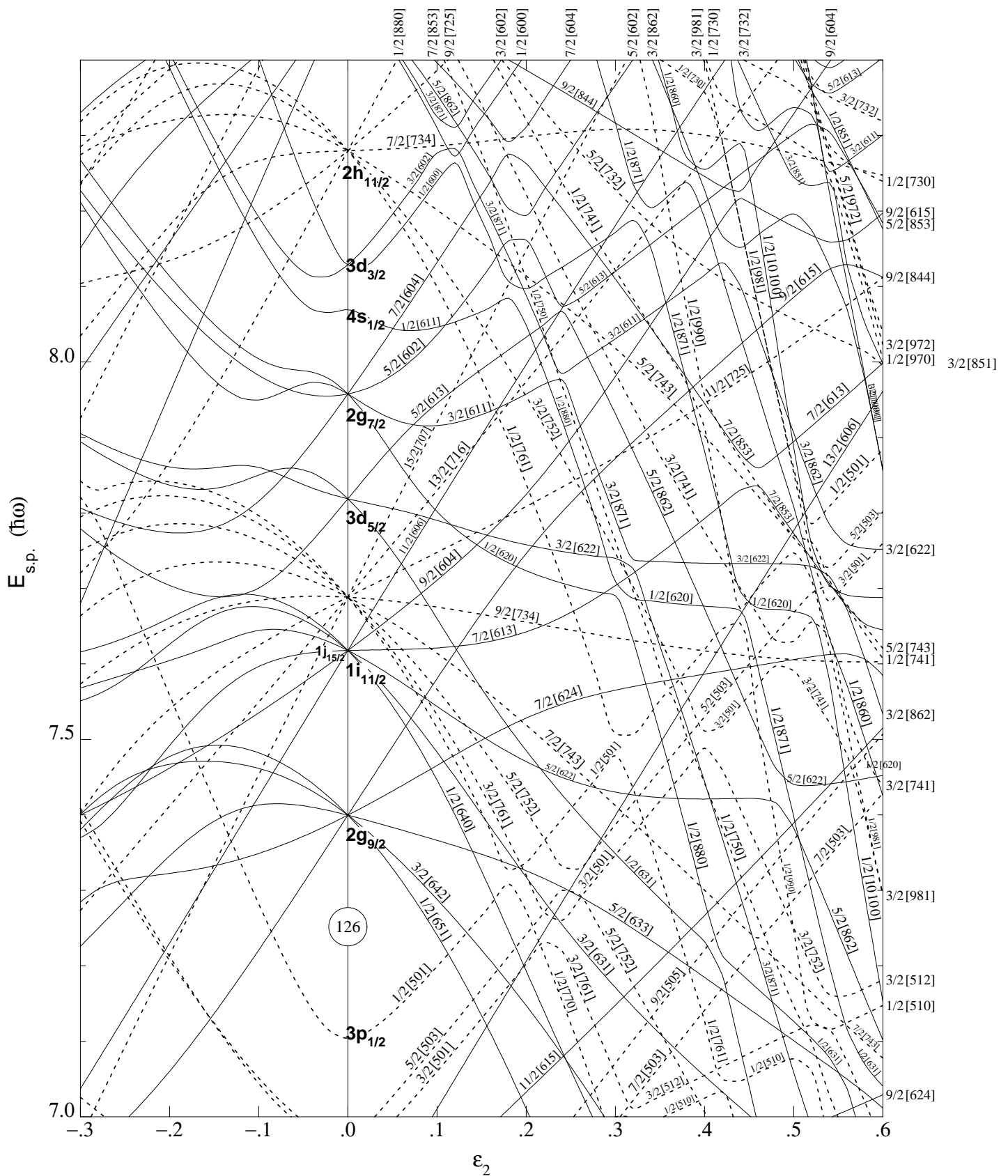


Figure 10. Nilsson diagram for neutrons, $N \geq 126$ ($\epsilon_4 = -\epsilon_2^2/6$).

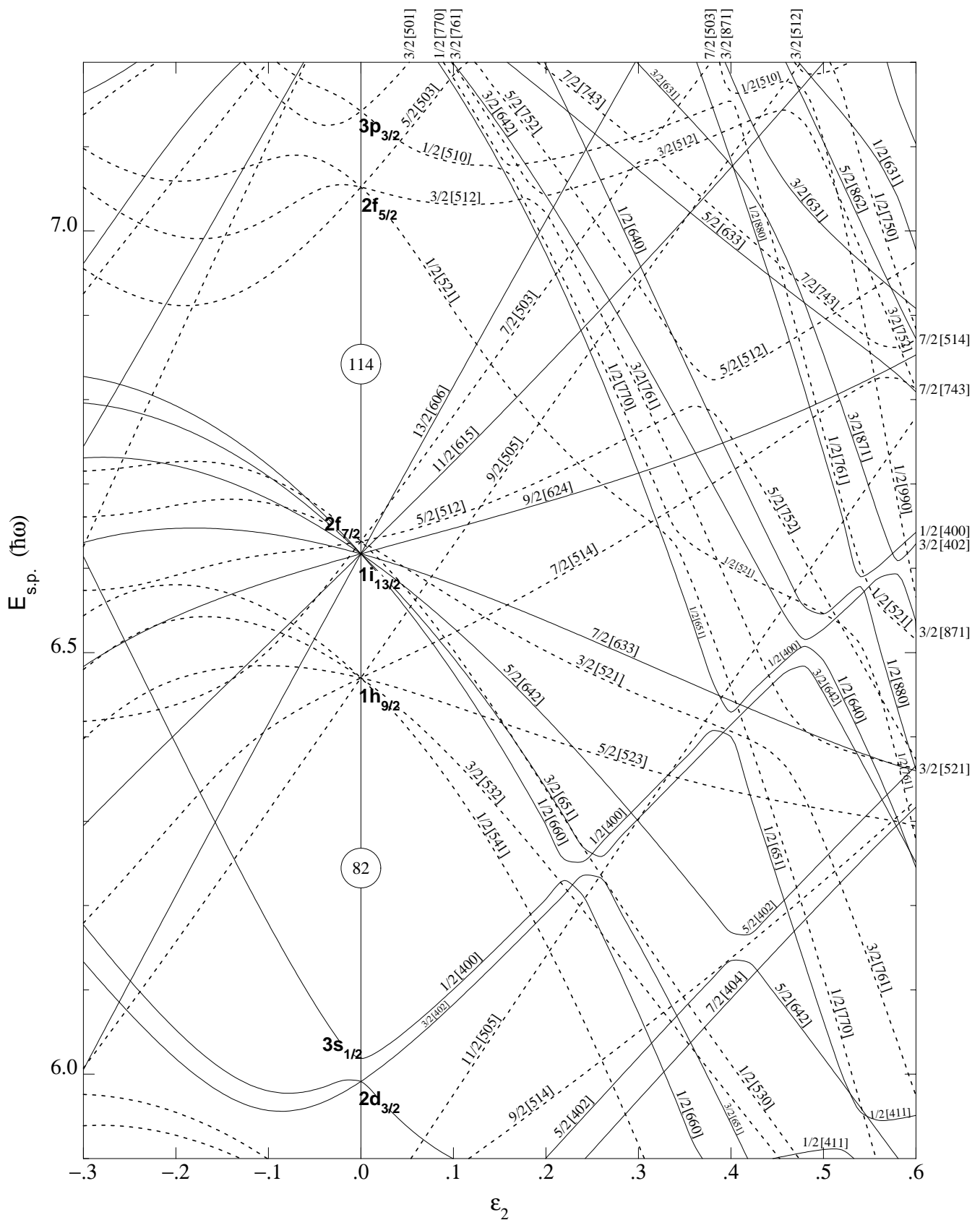


Figure 14. Nilsson diagram for protons, $Z \geq 82$ ($\epsilon_4 = -\epsilon_2^2/6$).

Additional quantities of interest for describing a rotational band include the rotational frequency

$$\hbar\omega(J) = \frac{E_\gamma((J+2)\rightarrow J) + E_\gamma(J\rightarrow(J-2))}{4} \text{ MeV}, \quad (18)$$

the kinetic moment of inertia

$$\mathcal{J}_1(J) = \frac{2J-1}{E_\gamma(J\rightarrow(J-2))} \hbar^2 \text{ MeV}^{-1}, \quad (19)$$

and the dynamic moment of inertia

$$\mathcal{J}_2(J) = \frac{4}{E_\gamma((J+2)\rightarrow J) - E_\gamma(J\rightarrow(J-2))} \hbar^2 \text{ MeV}^{-1}. \quad (20)$$

An experimental Routhian plot is often prepared to compare rotational bands with theory. This plot is restricted to sequences with $\Delta J=2$ when defining a band. The frequency parameter $\omega(J)$ is defined as

$$\omega(J) = \frac{E(J+1) - E(J-1)}{J_x(J+1) - J_x(J-1)}, \quad (21)$$

where the x-component of angular momentum J_x is

$$J_x(J) = \sqrt{(J+1/2)^2 - K^2}. \quad (22)$$

The experimental Routhian¹³ is defined by

$$E'(J) = 1/2[E(J+1)+E(J-1)] - \omega(J)J_x(J). \quad (23)$$

These Routhians are normally referenced to even-even nuclei where the quantities

$$e'(\omega) = E'(\omega) - E'_g(\omega), \quad (24)$$

$$j(\omega) = J_x(\omega) - J_{xg}(\omega).$$

Here $E'_g(\omega)$ and $J_{xg}(\omega)$ are the Routhian and the x-component of the angular momentum of the reference configuration, respectively. For an odd-A nucleus, the Routhian becomes

$$e'(A, \omega) = E'(A, \omega) + \Delta - 1/2[E'_g(A+1, \omega) + E'_g(A-1, \omega)], \quad (25)$$

where A is the mass number and Δ is the average even-odd mass difference.

4. Signature Splitting

The lowest energy state of each single-particle Nilsson configuration will have $J=K=\Omega$ ($\Omega \neq 1/2$). For each configuration there is a rotational band of levels where $K=\Omega$ and the energies are given by equation 4 with J taking on the values $K, K+1, K+2, K+3, \dots$. Coriolis and centrifugal forces introduce an additional term to the matrix element which involves a phase factor $\sigma=(-1)^{J+K}$ called the signature. This term alternates sign for successive values of J and implies that rotational bands with $K \neq 0$ divide into two families distinguished from each other by the quantum number σ . Bengtsson and Frauendorf¹³ have redefined the signature quantity for single particle states as $\alpha=\pm 1/2$, where α is an additive quantity where $r=e^{-i\pi\alpha}$. The total signature α_t for a configuration restricts the angular momentum to

$$J = \alpha_t \text{ mod } 2, \quad (26)$$

determining whether the band has odd or even particle number N , where

$$N = 2\alpha_t \text{ mod } 2. \quad (27)$$

For even-A nuclei, we obtain the 2-quasiparticle sequences:

$$\text{if } \alpha_t = 0 \text{ (} r = +1\text{), } J = 0, 2, 4, 6, \dots, \quad (28)$$

$$\text{if } \alpha_t = \pm 1 \text{ (} r = -1\text{), } J = 1, 3, 5, 7, \dots.$$

¹³ R. Bengtsson and S. Frauendorf, *Nucl. Phys.* **A327**, 139 (1979).

Similarly, for odd-A nuclei:

$$\text{if } \alpha_t = +1/2 \text{ (} r = -i \text{), } J = 1/2, 5/2, 9/2, \dots, \quad (29)$$

$$\text{if } \alpha_t = -1/2 \text{ (} r = +i \text{), } J = 3/2, 7/2, 11/2, \dots$$

An example of signature splitting is shown in Figure 15.

Collective particle configurations can also be discussed in terms of the alignment of the particle's intrinsic angular momentum with the angular momentum of the core. The "favored" (lowest energy) configuration occurs when these momenta are aligned to the maximum value. Decreasing the alignment by $1\hbar$ produces the "unfavored" configuration. These two configurations are analogous to the signature partners described above.

In octupole deformed nuclei, rotational states may be characterized by eigenvalues s of the simplex operator¹⁴ $J=PR^{-1}$ where R corresponds to reflection by 180° about an axis perpendicular to the symmetry axis and P is the parity operator. The spin J and parity p of a state in a rotational band which can be described by this "reflection" symmetry are related by $p=e^{-i\pi J}$. Accordingly, $s=\pm 1$ for even particle number (integral J), and $s=\pm i$ for odd particle number (half-integral J). These reflection-asymmetric deformations (octupole-quadrupole deformed) lead to bands of alternating parity, connected by enhanced $E1$ transitions, with levels nearly degenerate in energy for the same spin but opposite parity (parity doublets). Examples of parity doublets for an odd-particle system (^{221}Ra)¹⁵ and an even-particle system (^{224}Ac)¹⁶ are shown in Figure 16.

5. Superdeformation and Hyperdeformation

In 1968, Strutinski¹⁷ predicted a second minimum in the potential well for a deformed nucleus. This phenomenon was subsequently identified with fission isomers in the actinides, first observed by Polikanov *et al.*¹⁸ The associated shell gaps, calculated with an axially symmetric harmonic oscillator potential by Nix¹⁹ and by Bohr and Mottelson²⁰, are shown in Figure 17. These gaps occur with varying magic numbers for ratios of the semi-major to semi-minor axis of $3/2$ and 2 (superdeformation), and 3 (hyperdeformation). In 1986, Twin *et al.*^{21,22} reported the first evidence, for a superdeformed band in ^{152}Dy . Six superdeformed bands have been found in ^{152}Dy and are shown in Figure 18. Tentative evidence for a hyperdeformation in ^{152}Dy was reported by Galindo-Uribarri *et al.*²³ who observed a $\delta E_{\gamma} \approx \pm 30$ keV ridge structure in coincidence data for ^{152}Dy . Discrete transitions, possibly from a hyperdeformed band in ^{153}Dy , were reported by Viesti *et al.*²⁴.

¹⁴ W. Nazarewicz, P. Olanders, I. Ragnarsson, J. Dudek, and G.A. Leander, *Phys. Rev. Lett.* **52**, 1272 (1984).

¹⁵ J. Fernández-Niello, C. Mittag, F. Riess, E. Ruchowska, and M. Stalknecht, *Nucl. Phys.* **A531**, 164 (1991).

¹⁶ P.C. Sood, D.M. Headly, R.K. Sheline, and R.W. Hoff, *At. Data Nucl. Data Tables* **58**, 167 (1994).

¹⁷ V.M. Strutinski, *Nucl. Phys.* **A95**, 420 (1967); *ibid* **A122**, 1 (1968).

¹⁸ S.M. Polikanov, V.A. Druin, V.A. Karnaukhov, V.L. Mikheev, A.A. Pleve, N.K. Skobelev, G.M. Ter-Akopyan, and V.A. Fomichev, *Zhur. Eksptl. i Teoret. Fiz.* **42**, 1464 (1962); *Soviet Phys. JETP* **15**, 1016 (1962).

¹⁹ J.R. Nix, *Ann. Rev. Nucl. Sci.* **22**, 65 (1972).

²⁰ A. Bohr and B.R. Mottelson, *Nuclear Structure*, Vol. II, p. 591, Benjamin, New York (1975).

²¹ P.J. Twin, B.M. Nyako, A.H. Nelson, J. Simpson, M.A. Bentley, H.W. Cranmer-Gordon, P.D. Forsyth, D. Howe, A.R. Mokhtar, J.D. Morrison, J.F. Sharpey-Shafer, and G. Sletten, *Phys. Rev. Lett.* **57**, 811 (1986).

²² P.J. Dagnall, C.W. Beausang, P.J. Twin, M.A. Bentley, F.A. Beck, Th. Byrski, S. Clarke, D. Curien, G. Duchene, G. de France, P.D. Forsyth, B. Haas, J.C. Lisle, E.S. Paul, J. Simpson, J. Styczen, J.P. Vivien, J.N. Wilson, and K. Zuber, *Phys. Lett.* **B335**, 313 (1994).

²³ A. Galindo-Uribarri, H.R. Andrews, G.C. Ball, T.E. Drake, V.P. Janzen, J.A. Kuehner, S.M. Mullins, L. Persson, D. Prevost, D.C. Radford, J.C. Waddington, D. Ward, and R. Wyss, *Phys. Rev. Lett.* **71**, 231 (1993).

²⁴ G. Viesti, M. Lunardon, D. Bazzacco, R. Burch, D. Fabris, S. Lunardi, N.H. Medina, G. Nebbia, C. Rossi-Alvarez, G. de Angelis, M. De Poli, E. Fioretto, G. Prete, J. Rico, P. Spolaore, G. Vedovato, A. Brondi, G. La Rana, R. Moro, and E. Vardaci, *Phys. Rev.* **C51**, 2385 (1995).

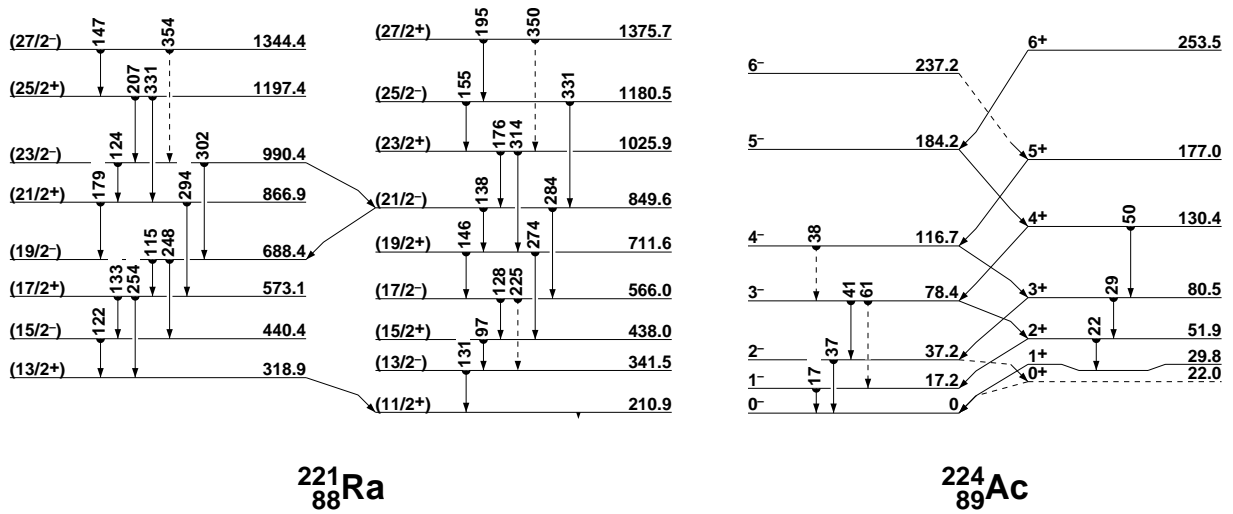


Figure 16. Examples of parity doublets arising from reflection asymmetry in ²²¹Ra and ²²⁴Ac.

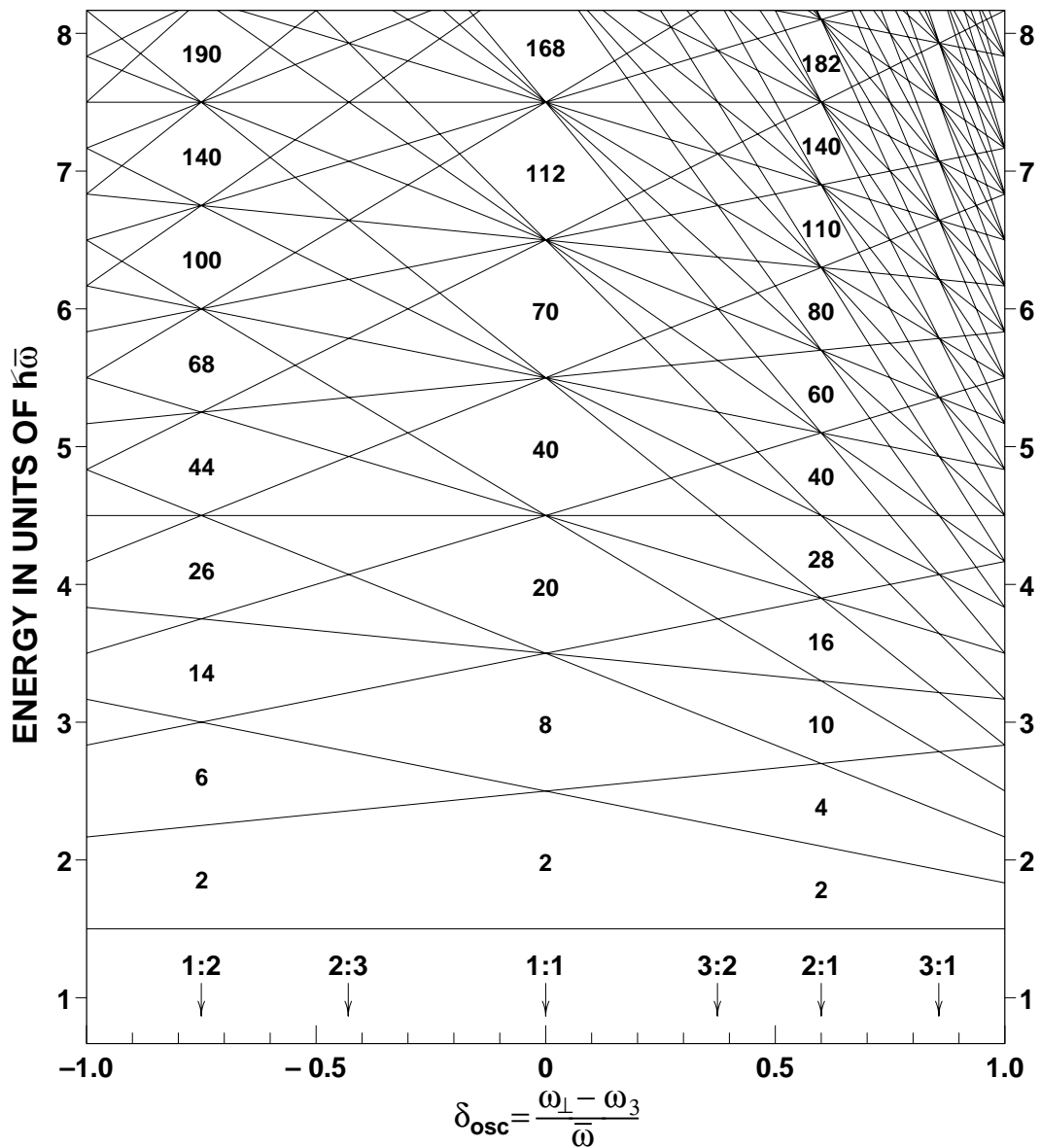
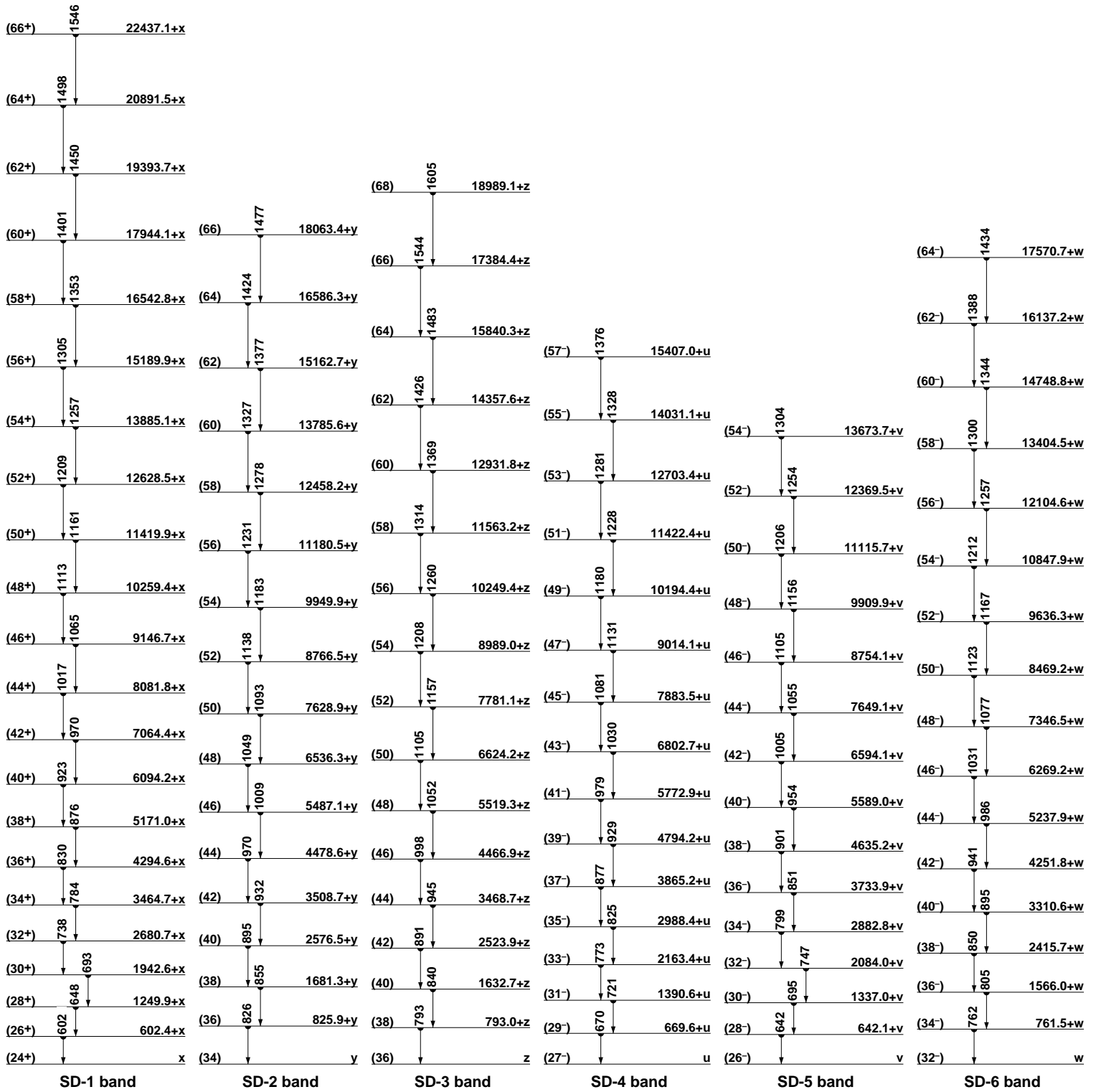


Figure 17. Single-particle level energies calculated for an axially symmetric harmonic oscillator (from reference 18).



$^{152}_{66}\text{Dy}$

Figure 18. Superdeformed rotational bands for ^{152}Dy